Int. J. Therm. Sci. (2001) 40, 564–570

S1290-0729(01)01244-3/FLA

Prandtl number effects for Marangoni convection over a flat surface

David M. Christopher*, Buxuan Wang

Thermal Engineering Department, Tsinghua University, Beijing, 100084 China

(Received 18 April 2000, accepted 31 July 2000)

Abstract — Marangoni convection, which is induced by the variation of the surface tension with temperature along a surface, influences crystal growth melts and other processes with liquid–vapor interfaces, such as boiling in both microgravity and in normal gravity in some cases. This paper presents a similarity solution for Marangoni flow over a flat surface for both the momentum equations and the energy equation assuming a developing boundary layer along a surface. Solutions are presented for the surface velocity, the total flow rate and the heat transfer for various temperature profiles and various Prandtl numbers. The analysis also shows how the heat transfer variation with Prandtl number changes for Prandtl numbers from much less than one to much greater than one. For large bubbles, the predicted boundary layer thickness would be less than the bubble diameter, so the curvature effects could be neglected and this analysis could be used as a first estimate of the effect of Marangoni flow around a vapor bubble. © 2001 Éditions scientifiques et médicales Elsevier SAS

Marangoni convection / similarity / liquid–vapor interface / microgravity / crystal melts

Nomenclature

a, d, h	exponents in similarity transformation	
A	temperature gradient coefficient	$K \cdot m^{-(k+1)}$
C_1	similarity transformation coefficient . .	m^a
C_2	similarity transformation coefficient . .	$s \cdot m^{(k-4)/3}$
$f(\eta)$	stream function similarity variable	
k	temperature gradient exponent	
$\dot{m}$	mass flow rate per unit width	$kg \cdot m^{-1} \cdot s^{-1}$
m	correlation coefficient	
n	correlation coefficient	
Ma	Marangoni number, equation (13)	
Nu	Nusselt number, equation (24)	
Pr	Prandtl number	
q''	heat flux	$W \cdot m^{-2}$
Re	Reynolds number, equation (16)	
T	temperature	K
u, v	velocities	$m \cdot s^{-1}$
x, y	coordinates	m

Greek symbols

α	thermal diffusivity	$m^2 \cdot s^{-1}$
δ	boundary layer thickness	m
η	location similarity variable	
η_δ	dimensionless momentum boundary layer thickness	
η_t	dimensionless thermal boundary layer thickness	
λ	thermal conductivity	$W \cdot m^{-1} \cdot K^{-1}$
μ	dynamic viscosity	$N \cdot s \cdot m^{-2}$
ν	kinematic viscosity	$m^2 \cdot s^{-1}$
θ	temperature similarity variable	
ρ	density	$kg \cdot m^{-3}$
σ	surface tension	$N \cdot m^{-1}$
ψ	stream function	$m^2 \cdot s^{-1}$

Subscripts

L	average over surface length
x	local value

1. INTRODUCTION

Marangoni flow induced by surface tension variations along a liquid surface causes undesirable effects in crystal growth melts in the same manner as buoyancy-induced

* Correspondence and reprints.
E-mail addresses: dmc@tsinghua.edu.cn (D.M. Christopher), bxwang@tsinghua.edu.cn (B. Wang).

natural convection [1]. These undesirable effects also occur in space-based crystal growth experiments since Marangoni flow occurs in microgravity as well as in earth gravity. Boiling tests in microgravity have shown that the effect of Marangoni flow is significant in microgravity and may be important in earth gravity as well [2, 3].

The numerous investigations of Marangoni flow in various geometries have been reviewed in the literature [4, 5]. Some of the papers most relevant to this work include the order-of-magnitude analysis of Marangoni flow given by Okano et al. [6] that gave the general trends for the variation of the Reynolds number with the Grashof number, Marangoni number, and Prandtl number. Hirata and his co-workers experimentally and numerically investigated Marangoni flow for various substances in geometries with flat surfaces relevant to this work [4, 6, 7]. Arafune and Hirata [8] presented a similarity analysis for just the velocity profile for Marangoni flow that is very similar to this derivation but the results are effectively limited to surface tension variations that are linearly related to the surface position. Slavtchev and Miladinova [9] presented similarity solutions for surface tension that varied as a quadratic function of the temperature as would occur near a minimum. Schwabe and Metzger [10] experimentally investigated Marangoni flow on a flat surface combined with natural convection in a unique geometry where the Marangoni effect and the buoyancy effect could be varied independently.

This paper presents a similarity solution for Marangoni flow over a flat surface due to an imposed temperature gradient. For an interface with evaporation or condensation at the surface, the temperature distribution along the interface is primarily a function of the vapor temperature and the heat transfer coefficient rather than the Marangoni flow. For example, Christopher and Wang [3] showed that the calculated temperature distribution in a vapor bubble attached to a surface and in the liquid surrounding the bubble was primarily due to the heat transfer through the vapor rather than in the liquid region and the temperature variation along the surface was not linear but could be described by a power-law function as proposed here.

The objective of this analysis is to develop a simplified analysis of the temperature distribution along a surface with an imposed temperature distribution which would most likely be due to evaporation and condensation at the interface. The analysis assumes that the surface tension varies linearly with temperature but the temperature variation is a power-law function of the location. In addition, the analysis assumes that a boundary layer develops along the surface due to the coupled Marangoni flow. The results for the heat transfer are then correlated as a function of Prandtl number. The analytical results can also be used to evaluate numerical solutions of the complete Navier–Stokes and energy equations for boundary conditions that meet the specified conditions.

2. THEORETICAL ANALYSIS

Unlike the Boussinesq effect in buoyancy flow, the Marangoni effect acts as a boundary condition on the governing equations for the flow field. For laminar boundary layer flow over a flat plate, the Navier–Stokes equations can be reduced to the continuity equation and the boundary layer momentum equation [4]:

$$\frac{\partial u}{\partial x}+\frac{\partial v}{\partial y}=0 \tag{1}$$

$$u\frac{\partial u}{\partial x}+v\frac{\partial u}{\partial y}=\nu\frac{\partial^2 u}{\partial y^2} \tag{2}$$

The boundary layer energy equation is

$$u\frac{\partial T}{\partial x}+v\frac{\partial T}{\partial y}=\alpha\frac{\partial^2 T}{\partial y^2} \tag{3}$$

The corresponding boundary conditions at the surface are

$$\begin{aligned}\mu\frac{\partial u}{\partial y}\bigg|_{y=0}&=-\frac{\mathrm{d}\sigma}{\mathrm{d}T}\frac{\partial T}{\partial x}\bigg|_{y=0}\\ v(x,0)&=0\\ T(x,0)&=T(0,0)+Ax^{k+1}\end{aligned} \tag{4}$$

Far from the surface, the boundary conditions are

$$u(x,\infty)=0 \tag{5a}$$

$$T(x,\infty)=T_\infty=T(0,0) \tag{5b}$$

Using the standard definition of the stream function, similarity variables can be introduced as

$$\begin{aligned}\eta&=C_1x^d y\\ f(\eta)&=C_2x^a\psi(x,y)\\ \theta(\eta)&=\frac{(T(x,y)-T(0,0))x^h}{A}\end{aligned} \tag{6}$$

so the governing equations can then be written as

$$\begin{aligned}f'''&=f'^2(d-a)+aff''\\ \theta''&=Pr\left(af\theta'-hf'\theta\right)\end{aligned} \tag{7}$$

where the coefficients are defined as

$$C_1 = \sqrt[3]{\frac{(\mathrm{d}\sigma/\mathrm{d}T)A\rho}{\mu^2}}$$
$$C_2 = \sqrt[3]{\frac{\rho^2}{(\mathrm{d}\sigma/\mathrm{d}T)A\mu}} \tag{8}$$

For similarity, the exponents are related to k in equation (4) by

$$d = \frac{k-1}{3}$$
$$a = \frac{-2-k}{3} \tag{9}$$
$$h = -1-k$$

The momentum equation boundary conditions are

$$f(0) = 0$$
$$f''(0) = -1 \tag{10}$$
$$f'(\infty) = 0$$

The energy equation boundary conditions are

$$\theta(0) = 1$$
$$\theta(\infty) = 0 \tag{11}$$

The surface velocity is given by

$$u(x,0) = \sqrt[3]{\frac{((\mathrm{d}\sigma/\mathrm{d}T)A)^2}{\rho\mu}} f'(0) x^{(2k+1)/3} \tag{12}$$

The temperature gradient coefficient can be defined in terms of the total temperature difference along a surface of length L as $A = \Delta T/L^{k+1}$ so the Marangoni number can then be defined for a general temperature profile as

$$Ma_{\mathrm{L}} = \frac{(\mathrm{d}\sigma/\mathrm{d}T)(\Delta T/L^{k+1})L^{k+2}}{\mu\alpha}$$
$$= \frac{(\mathrm{d}\sigma/\mathrm{d}T)\Delta T L}{\mu\alpha} \tag{13}$$

The Reynolds number defined in terms of the surface velocity is then related to the Marangoni number as

$$Re_{\mathrm{L}} = \frac{u(x,0)L}{\nu} = f'(0)\, Ma_{\mathrm{L}}^{2/3} Pr^{-2/3} \tag{14}$$

The total mass flow in the boundary layer per unit width is given by

$$\dot{m} = \int_0^\infty \rho u \, \mathrm{d}y = \sqrt[3]{\frac{\mathrm{d}\sigma}{\mathrm{d}T} A\rho\mu}\, x^{(k+2)/3} f(\infty) \tag{15}$$

which can be written in dimensionless form as

$$\overline{Re}_{\mathrm{x}} = \frac{\rho\bar{u}\delta}{\mu} = f(\infty)\, Ma_x^{1/3} Pr^{-1/3} \tag{16}$$

The similarity transformation used here for the momentum equation differs in several ways from that used by Arafune and Hirata [8]. Besides slightly different definitions of the similarity variables, the most important difference is that the present derivation is based on a general form of the temperature variation on the surface. The results of Arafune and Hirata [8] are only useful for a linear variation of the surface tension with location. The current derivation is also extended to include the energy equation.

The similarity analysis is based on the boundary layer equations which assume that the transverse derivatives of the velocity and temperature are much larger than their axial derivatives and that the axial velocity is much larger than the transverse velocity. Analysis of the similarity transformation shows that both are true if

$$C_1 L^{(k+2)/3} = \sqrt[3]{\frac{(\mathrm{d}\sigma/\mathrm{d}T)A\rho L^{k+2}}{\mu^2}}$$
$$= Ma_{\mathrm{L}}^{1/3} Pr^{-1/3} \gg 1 \tag{17}$$

The numerical results can be used to show that the boundary layer assumptions hold within the momentum boundary layer for $Ma_{\mathrm{L}}/Pr > 10^6$ and for $k \leq 2$.

3. RESULTS AND DISCUSSION

3.1. Similarity results

The governing equations (7) were solved numerically using the fourth-order Runge–Kutta method with at least 20 000 steps. The shooting method was used to determine the unknown boundary conditions at $\eta = 0$, $f'(0)$ for the momentum equation and $\theta'(0)$ for the energy equation. The maximum value for the independent variable η, which was a function of the Prandtl number, was always chosen to be at least 4 times the maximum boundary layer thickness. The minimum value that could be used for the momentum equation was $\eta = 20$ which was sufficient for the energy equation for Prandtl numbers greater than 2. For Prandtl numbers less than 2, the thermal boundary layer thickness and, hence, the maximum value of η were much greater. The results presented in the following section were all independent of the number of steps and the maximum value of η.

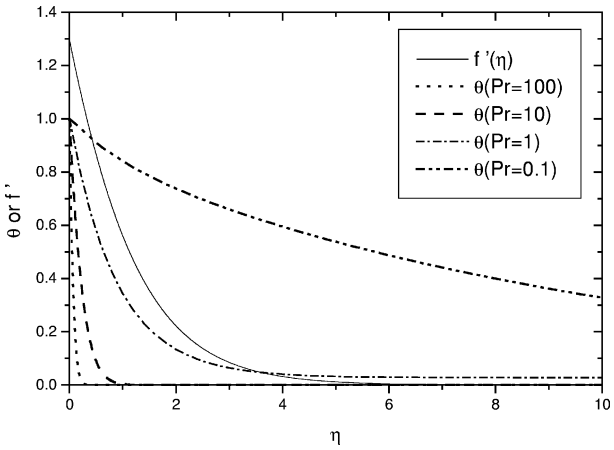

Figure 1. Velocity and temperature profiles for $k = 0$.

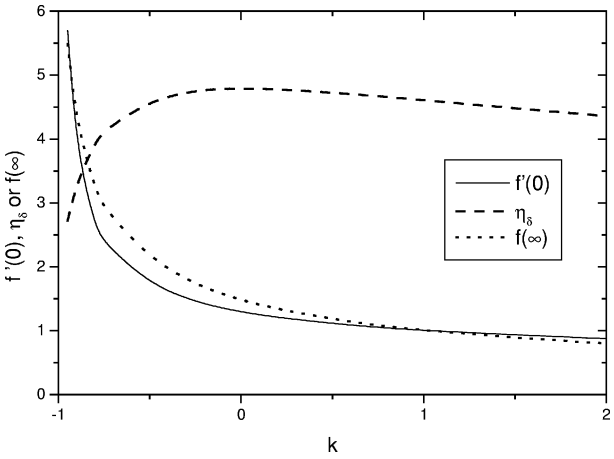

Figure 2. Variations of surface velocity, boundary layer thickness and flow rate for various temperature gradient exponents.

The similarity stream function f is a function of the exponent k, while the temperature function θ is a function of both k and the Prandtl number. The governing equations (7) were solved subject to the boundary conditions in equations (10) and (11) for various values of k and Pr. Typical velocity and temperature profiles are given in *figure 1* for several representative values of the Prandtl number and for $k = 0$ which is a linear surface temperature profile. The thickness of the thermal boundary layer increased with increasing Prandtl number as expected.

The variations of the surface velocity, the boundary layer thickness and the total flow rate in the boundary layer are given as functions of k in *figure 2*, of which $k = 0$ refers to a linear profile, $k = 1$ is quadratic, while $k = -0.5$ would be a temperature variation relative to the square root of x. The minimum value of k is -1, which

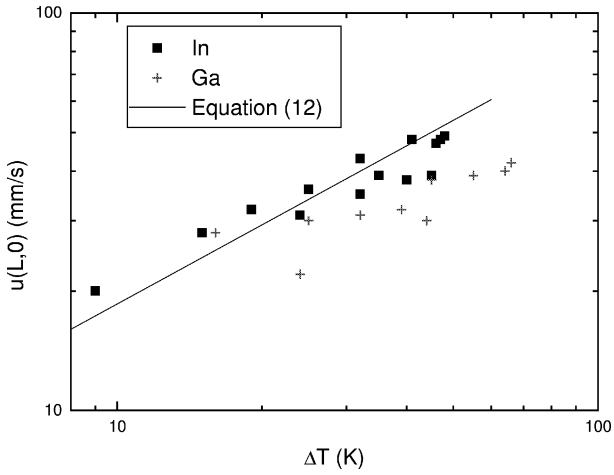

Figure 3. Comparison of experimental results from [7] with the predicted surface velocities.

would result in no temperature variation on the surface and, thus, no Marangoni flow. The momentum boundary layer thickness was defined as usual as the point where the velocity is 1 % of the surface velocity. The velocity for small values of k is greater because for a fixed total temperature difference across the surface, the profile for a small value of k is steeper near the leading edge which provides more flow. For larger values of k, the slope of the temperature profile is larger near the trailing edge where the boundary layer is thicker and the additional acceleration of the flow has less effect. The mass flow rate follows the same trend. The boundary layer thickness is greatest for the uniformly increasing temperature profile, $k = 0$. For k greater than or less than 0, the temperature profile over part of the plate is relatively flat, so the flow does not accelerate much in that region and the boundary layer does not grow. The similarity solution could be used to calculate the Marangoni flow over a curved surface if the boundary layer thickness, which varies from 3 to 5 for the range in *figure 2* and is 4.79 for the linear temperature profile, is small compared to the curvature. The temperature distribution along the bubble surface calculated by Christopher and Wang [3] varied rapidly at first and then more slowly along a curve that could be described by equation (4) with $k \approx -0.9$. Therefore, the results presented here could be used at least as an initial estimate of the boundary layer effect due to Marangoni flow around a vapor bubble in some cases.

The surface velocities are compared to the velocities measured by Arafune et al. [7] for gallium and indium in a shallow pool in *figure 3*. The similarity results agree well with the measured velocities for indium. Okano et al. [6] showed that the Reynolds number should vary

as the two-thirds root of the Marangoni number for large Reynolds numbers. The similarity and experimental results agree with their analysis that the surface velocity should vary as the two-thirds root of the temperature difference. The measured velocities for gallium do not agree as well with the analysis and do not seem to vary as the two-thirds power of the temperature perhaps due to the buoyancy effects and the effect of the entire recirculating flow field in the pool.

3.2. Prandtl number effects

Two representative temperature profiles for $k = 0$ and small Prandtl numbers are shown in *figure 4*. The similarity results are compared with an approximate analysis of the energy equation for small Prandtl numbers where the thermal boundary layer thickness is much greater than the momentum boundary layer thickness. Therefore, over most of the domain, $f'(\eta)$ is equal to zero and $f(\eta)$ is equal to $f(\infty)$ so the energy equation given in equation (7) can be approximated by

$$\theta'' = Pr\, a f(\infty)\theta' \tag{18}$$

The solution of equation (18) subject to the boundary conditions given in equation (11)

$$\theta(\eta) = \mathrm{e}^{-Pr((k+2)/3) f(\infty)\eta} \tag{19}$$

is compared to the similarity solution in *figure 4*. The temperature gradient at the surface for small Prandtl numbers would then vary as

$$\theta'(0) = -Pr\left(\frac{k+2}{3}\right) f(\infty) \tag{20}$$

Therefore, for small Prandtl numbers the surface temperature gradient would be expected to be proportional to the Prandtl number for a given surface temperature variation.

For large Prandtl numbers, the thermal boundary layer thickness is much thinner than the momentum boundary layer thickness, so the energy equation can be approximated by assuming that $f(\eta)$ is essentially zero and that $f'(\eta)$ is essentially $f'(0)$ for small η. Therefore, for large Prandtl numbers, the energy equation can be approximated by

$$\theta'' = Pr(k+1) f'(0)\theta \tag{21}$$

which has the solution

$$\theta(\eta) = \mathrm{e}^{-\sqrt{Pr(k+1) f'(0)}\,\eta} \tag{22}$$

The surface temperature gradient for large Prandtl numbers would then be approximated by

$$\theta'(0) = -\sqrt{Pr(k+1) f'(0)} \tag{23}$$

The variation of the surface temperature gradient as a function of the Prandtl number and the temperature gradient exponent is shown in *figure 5* for a wide range of Prandtl numbers. The slope of the curve on the logarithmic axes is equal to one for small Prandtl numbers and is equal to 0.5 for large Prandtl numbers. Equation (23) for large Prandtl numbers coincides with the full similarity solution for $Pr > 10$, but equation (20) for small Prandtl numbers is somewhat less than the

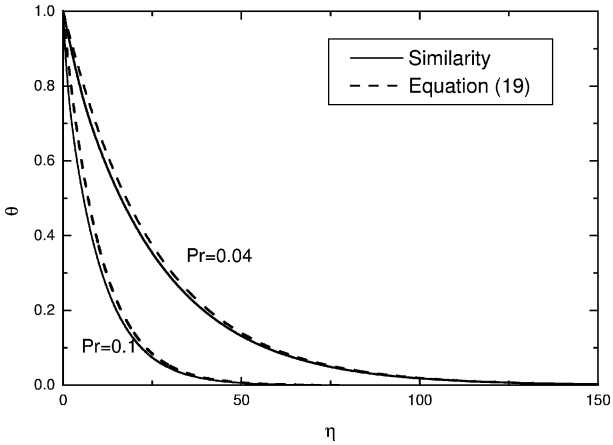

Figure 4. Temperature distributions for small Prandtl numbers for $k = 0$.

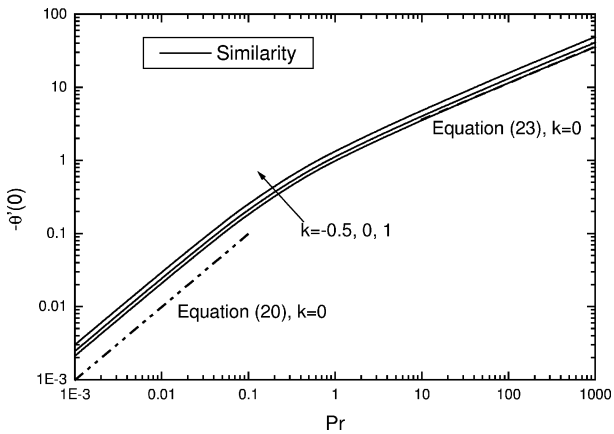

Figure 5. Surface temperature gradient for various conditions.

similarity solution even for $Pr = 0.001$, *figure 5*. The error in equation (20) is because the assumptions on the values of $f(\eta)$ and $f'(\eta)$ for small Prandtl numbers are not accurate near the surface; therefore, the value of the surface temperature gradient predicted by equation (20) is not accurate although the form of the equation is correct.

The local Nusselt number is

$$Nu_x = \frac{q''(x)x}{\lambda(T(x,0) - T(x,\infty))} = -C_1\theta'(0)x^{(k+2)/3} \quad (24)$$

For small Prandtl numbers, the Nusselt number is

$$Nu_x = -Ma_x^{1/3}Pr^{-1/3}\left(\frac{x}{L}\right)^{(k+2)/3}\theta'(0) \propto Ma_x^{1/3}Pr^{2/3}\left(\frac{x}{L}\right)^{(k+2)/3}\frac{k+2}{3}f(\infty) \quad (25)$$

For large Prandtl numbers, the Nusselt number is

$$Nu_x = -Ma_x^{1/3}Pr^{-1/3}\left(\frac{x}{L}\right)^{(k+2)/3}\theta'(0) \propto Ma_x^{1/3}Pr^{1/6}\left(\frac{x}{L}\right)^{(k+2)/3}\sqrt{(k+1)f'(0)} \quad (26)$$

Therefore, the slope of the Nusselt number is proportional to the two-thirds power of the Prandtl number for small Prandtl numbers and is proportional to the one-sixth power of the Prandtl number for large Prandtl numbers as the thermal boundary layer becomes thinner than the velocity boundary layer. In addition, the coupling of the temperature and flow fields means that the exponent k and the values of $f(\eta)$ and $f'(\eta)$ are functions of the Marangoni and Prandtl numbers which will introduce additional Marangoni and Prandtl number effects.

4. CONCLUSIONS

Marangoni flow has been analyzed for boundary layer flow over a flat surface with an imposed temperature gradient. The governing equations were solved using a similarity analysis applicable to both linear and nonlinear temperature gradients. For a liquid pool heated at both ends, the surface temperature gradient would only be expected to be linear for very low Prandtl number fluids where the conduction in the fluid is much greater than the convection heat transfer. The predicted surface velocities agree well with measured values for a shallow pool of liquid indium [7]. The numerical results show that the boundary layer assumptions hold within the momentum boundary layer for $Ma_L/Pr > 10^6$ and for $k \leq 2$.

The velocity and temperature field distributions are given by the results for boundary layer flow with power-law variations of the surface temperature gradient. Equations are given for the surface velocity, the total mass flow rate and the heat flux at the interface as functions of the Marangoni, Prandtl and Reynolds numbers, the exponent k and the location. For $k = 0$, the analysis agrees with previous results for a linear temperature gradient [6] that the Reynolds number based on the surface velocity varies as the two-thirds power of the Marangoni number. The variation of the temperature gradient at the surface is given for a wide range of Prandtl numbers. For small Prandtl numbers, the analysis shows that the Nusselt number is proportional to the two-thirds power of the Prandtl number. For large Prandtl numbers, the Nusselt number is proportional to the one-sixth power of the Prandtl number.

The results can also be used to calculate the Marangoni flow and the resulting heat transfer for flow over curved surfaces when the curvature is much greater than the boundary layer thickness. The predicted temperature profile along the bubble interface for a vapor bubble in a liquid pool with condensation and evaporation at the interface [3] could be described with a power-law variation of the temperature as described in this paper. The analytical results can also be used as an analytical solution to evaluate numerical solutions of the complete Navier–Stokes and energy equations for boundary conditions that meet the specified conditions.

Acknowledgement

The project was financially supported by the National Natural Science Foundation of China with grant number 59995550-3.

REFERENCES

[1] Eyer A., Leist H., Nitsche R., Floating zone growth of silicon under microgravity in a sounding rocket, J. Crystal Growth 71 (1985) 173–182.

[2] Straub J., The role of surface tension for two-phase heat and mass transfer in the absence of gravity, Experiment. Therm. Fluid Sci. 9 (1994) 253–273.

[3] Christopher D., Wang B., Marangoni convection around a bubble in microgravity, heat transfer, in: Lee J.S. (Ed.), Proceedings of the 11th International Heat Transfer Conference, Vol. 3, Taylor & Francis, Levittown, 1998, pp. 489–494.

[4] Arafune K., Hirata A., Interactive solutal and thermal Marangoni convection in a rectangular open boat, Numer. Heat Tran. Part A 34 (1998) 421–429.

[5] Croll A., Muller-Sebert W., Nitsche R., The critical Marangoni number for the onset of time-dependent convection in silicon, Mater. Res. Bull. 24 (1989) 995–1004.

[6] Okano Y., Itoh M., Hirata A., Natural and Marangoni convections in a two-dimensional rectangular open boat, J. Chem. Engrg. Japan 22 (1989) 275–281.

[7] Arafune K., Sugiura M., Hirata A., Investigation of thermal Marangoni convection in low and high Prandtl number fluids, J. Chem. Engrg. Japan 32 (1999) 104–109.

[8] Arafune K., Hirata A., Thermal and solutal Marangoni convection in In–Ga–Sb system, J. Crystal Growth 197 (1999) 811–817.

[9] Slavtchev S., Miladinova S., Thermocapillary flow in a liquid layer at minimum in surface tension, Acta Mechanica 127 (1998) 209–224.

[10] Schwabe D., Metzger J., Coupling and separation of buoyant and thermocapillary convection, J. Crystal Growth 97 (1989) 23–33.